

Persistent Luminescence of Tenebrescent $\text{Na}_8\text{Al}_6\text{Si}_6\text{O}_{24}(\text{Cl},\text{S})_2$: Multifunctional Optical Markers

Isabella Norrbo,[†] Pawel Gluchowski,[‡] Petriina Paturi,[§] Jari Sinkkonen,[†] and Mika Lastusaari^{*,†,||}

[†]Department of Chemistry, University of Turku, FI-20014 Turku, Finland

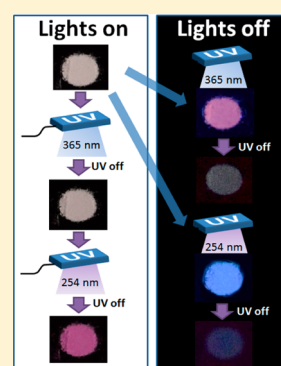
[‡]Institute of Low Temperature and Structure Research Polish Academy of Sciences, PL-50422 Wroclaw, Poland

[§]Department of Physics and Astronomy, Wihuri Physical Laboratory, University of Turku, FI-20014 Turku, Finland

^{||}Turku Centre for Materials and Surfaces (MatSurf), FI-20014 Turku, Finland

S Supporting Information

ABSTRACT: $\text{Na}_8\text{Al}_6\text{Si}_6\text{O}_{24}(\text{Cl},\text{S})_2$ materials were prepared with a solid state reaction. The products were studied using X-ray powder diffraction, reflectance measurements as well as X-ray fluorescence, conventional and persistent luminescence, nuclear magnetic resonance, and electron paramagnetic resonance spectroscopies. All materials containing sulfur showed purple tenebrescence, which persisted 2 days in a lit room at room temperature. Considerable blue persistent luminescence peaking at 460 nm and lasting for 1 h was obtained, as well. Persistent luminescence was obtained with irradiation at 365 nm, while tenebrescence required 254 nm. The materials show great promise as low-cost multifunctional optical markers.



1. INTRODUCTION

Persistent luminescence is a phenomenon involving the sustained release of absorbed energy as visible light after the removal of the excitation source for which radiation with the energy of blue light or higher can be used. There is no official definition for the length of luminescence in order to classify as persistent luminescence, but a duration of minutes or hours is usually required. In addition to persistent luminescence, the phenomenon has various other names such as afterglow and long persistent phosphorescence.¹ Since persistent luminescence is based on the trapping of charge carriers and their slow release stimulated by thermal energy, it is thermally stimulated luminescence rather than phosphorescence. Nowadays, the best persistent luminescence materials such as $\text{Sr}_2\text{MgSi}_2\text{O}_7\text{:Eu}^{2+},\text{Dy}^{3+2}$ (Sr åkermanite) or $\text{SrAl}_2\text{O}_4\text{:Eu}^{2+},\text{Dy}^{3+3}$ (Sr krotite) can emit visible light in excess of 24 h in the dark. These materials are widely employed in commercial applications such as self-lit exit signs. There are also materials that emit persistent luminescence in the near-infrared with $\text{Zn}_3\text{Ga}_2\text{Ge}_2\text{O}_{10}\text{:Cr}^{3+}$ being the most efficient one having a 360 h duration.⁴ Most persistent luminescence materials studied or used commercially contain expensive rare earths (lanthanides) and/or environmentally undesired heavy metals. Thus, there is a need to develop new materials without these drawbacks. As an answer to this need, we demonstrate here for the first time that synthetic hackmanites $\text{Na}_8\text{Al}_6\text{Si}_6\text{O}_{24}(\text{Cl},\text{S})_2$ can function as efficient persistent luminescence materials, without any rare earth or heavy metal doping.

Tenebrescence or reversible photochromism as a phenomenon is closely related to persistent luminescence. It also involves the trapping of charge carriers and their sustained release by thermal or optical energy. The trapping of electrons creates a color center, which absorbs visible light until the electron escapes from the trap as a result of thermal or optical stimulation.⁵ Alkali metal halides and other materials such as silver halides, alkaline earth fluorides, magnesium, and titanium oxide show tenebrescence.⁵ Moreover, there are a number of minerals that exhibit tenebrescence {e.g., hackmanite ($\text{Na}_8\text{Al}_6\text{Si}_6\text{O}_{24}(\text{Cl},\text{S})_2$),⁵ tugtupite ($\text{Na}_4\text{AlBeSi}_4\text{O}_{12}\text{Cl}$),⁶ and scapolite [$(\text{Na},\text{Ca})_4(\text{Al},\text{Si})_3\text{Si}_6\text{O}_{24}(\text{Cl},\text{CO}_3,\text{SO}_4)$]}.⁷ Materials with this property are most commonly used in color changing eyeglasses sensitive to the amount of sunlight.⁸ In this paper, we present for the first time synthetic hackmanites that show tenebrescence simultaneously with persistent luminescence.

The hackmanite structure is based on that of sodalite.⁹ It crystallizes in the cubic space group $P\bar{4}3n$ (no. 218) with the unit cell axis length of 8.877(2) Å.⁸ The structure consists of a framework built up of four- and six-membered rings of alternating AlO_4 and SiO_4 tetrahedra. This framework has large cavities containing Cl^- and Na^+ ions forming $(\text{Na}_4\text{Cl})^{3+}$ entities. From these entities, Na is coordinated to three O^{2-} ions from the framework and one Cl^- . In hackmanite, some of the Cl^- ions have been substituted by sulfur-containing ions, such as S_2^{2-} , SO_3^{2-} , or SO_4^{2-} .^{8,10}

Received: March 12, 2015

Published: August 6, 2015



The tenebrescence of natural as well as synthetic hackmanite has been reported by many authors upon exposure to UV or radiation with higher energy (see, for example, refs 5, 8, and 11–13). In these reports, the color ranges from pink, red, and purple to blue. According to Williams et al.,¹⁴ the color of tenebrescence in sodalites depends on the size of the anion vacancy in such a way that there is a positive linear dependency between the cubic unit cell a axis length and the absorption maximum. Once showing tenebrescence, the materials' reddish and purple colors may last for seconds¹² to minutes⁸ under normal ambient conditions with lights on. The blue color can be obtained by exposing natural hackmanite for some hours by UV radiation, but for synthetic materials, only the purple color is obtained even with prolonged exposure times. The blue color can persist for weeks in ambient temperature and light.⁸ In the dark, none of the colors show fading. Currently, it is agreed that the tenebrescence is due to long-lived F centers (color centers) formed from anion vacancies [i.e., $(\text{Na}_4\Box)^{4+}$ entities (where \Box denotes an anion vacancy)], that trap electrons originating from nearby S_2^{2-} groups⁸ or S_x^{2-} groups in general.¹⁵

According to Gaft et al.,⁶ natural hackmanites show red emission peaking at ca. 680 nm. This is attributed to the $^2\Pi_u \rightarrow ^2\Pi_g$ transition of the S_2^- ion. Kirk¹² reported this emission also for synthetic hackmanites produced from natural sodalites. Some natural hackmanite specimens also show blue emission around 450 nm with a long decay time of several seconds.⁶ This emission has been assigned to be due to the $^3\text{P}_{0,1} \rightarrow ^1\text{S}_0$ transitions of s^2 type ions such as Pb^{2+} , Tl^+ , Sn^{2+} , and Sb^{2+} . However, the exact emitting center has not been verified.

In this work, we investigated synthetic hackmanites $\text{Na}_8\text{Al}_6\text{Si}_6\text{O}_{24}(\text{Cl},\text{S})_2$ and the effect of the Cl and S content on the tenebrescence and luminescence of the materials. The sulfur content was chosen so as to correspond to that found in the natural hackmanites,¹⁵ and the vacancy concentration was kept constant. To the knowledge of the authors, the present paper is the first one to report persistent luminescence for $\text{Na}_8\text{Al}_6\text{Si}_6\text{O}_{24}(\text{Cl},\text{S})_2$.

2. EXPERIMENTAL SECTION

2.1. Sample Preparation. The hackmanite samples were prepared with a solid state reaction using stoichiometric amounts of Zeolite A (Sigma-Aldrich, product no. 96096), NaCl (J. T. Barker, 99.5%), and Na_2SO_4 (E. Merck, 99%) as the starting materials. The impurity contents of the starting materials are listed in Tables S1 and S2.

Zeolite A was first dried at 500 °C for 1 h. The initial mixture was heated at 850 °C in air for 48 h. The product was then freely cooled down to room temperature and ground. Finally, the product was reheated at 850 °C for 2 h under a flowing 12% H_2 + 88% N_2 atmosphere. When varying the composition, we assumed that sulfur is present as S^{2-} , which then would result in the stoichiometry $\text{Na}_8\text{Al}_6\text{Si}_6\text{O}_{24}(\text{Cl}_{2-2x-y}\text{S}_x\Box)_2$. The vacancy (denoted with \Box) concentration was kept constant at $y = 0.2$, and the x value was 0.0, 0.1, 0.2, 0.3, and 0.4. However, it is not possible to judge whether the sulfur is present as S^{2-} , S_2^{2-} , or even S_2^- . Thus, in the text below, we use the molar ratio $n(\text{S}):n(\text{Cl})$ for identifying the samples because it is independent of the valences.

2.2. Characterization. The structure and purity of the products was checked by routine room temperature X-ray powder diffraction (XPD) measurements using a Huber G670 detector and copper $K_{\alpha 1}$ radiation ($\lambda = 1.54060$ Å). Rietveld refinements¹⁶ were carried out to determine the unit cell volumes. The FullProf program¹⁷ was used. The NaCl impurity content was determined from the diffraction intensities employing the RIR (reference intensity ratio) method¹⁸ with the I/I_c values of NaCl and sodalite.¹⁹ The sample compositions were further probed with X-ray fluorescence spectroscopy (XRF)

using the PANalytical epsilon 1 apparatus with its internal Omnic calibration.

The color of the materials was investigated with reflectance measurements under illumination from a 60 W incandescent light bulb located 20 cm above the sample. This was considered as far enough not to heat the sample. The samples were irradiated with a hand-held 4 W UV lamp (UVP UVGL-25 with 254 and 365 nm lamps) for 5 min to induce the color change. The reflectance spectra were then collected with an optical fiber and recorded with an Avantes AvaSpec-2084 × 14 spectrometer using a data collection time of 800 ms for initial color measurements (ca. 15 s after switching off the UV lamp) and 400 ms for the fading measurements.

The UV excited luminescence and persistent luminescence properties were studied at room temperature using a Varian Cary Eclipse Fluorescence Spectrophotometer equipped with a Hamamatsu R928 photomultiplier and a 15 W xenon lamp. For the UV excited spectra, the samples were excited with the internal light source. For the measurements, a delay of 0.1 ms was used together with a 5 ms gate time. For the persistent luminescence measurements, the samples were irradiated with the hand-held UV lamp for 30 min at room temperature. The first measurement was carried out 1 min after ceasing the irradiation and then the emission spectrum was saved every minute up to 1 h. Each measurement took 4 s. The luminescence intensity was calculated by integrating the area under the whole emission curve. The fading times were calculated taking into account the change of the intensity of persistence luminescence (by integrating the area under the whole emission curve) as a function of time.

The local structure around Cl^- ions was studied with solid state ^{35}Cl MAS NMR spectroscopy. The data were recorded at room temperature with a Bruker AV400 apparatus using 12 000 Hz spinning and a 0.1 s relaxation time. The ppm scale was calibrated against 1 molar aqueous NaCl, whose resonance was assigned to 0.0 ppm.

The presence of unpaired electrons was probed with EPR spectroscopy at 20 K using a homemade X band EPR spectrometer with a frequency of ca. 9.03 GHz. A microwave power of ca. 1 mW and a modulation field of 100 kHz were used.

3. RESULTS AND DISCUSSION

3.1. Phase Purity and Composition. X-ray powder diffraction measurements were carried out for each material in order to analyze their purity. The diffraction patterns (Figure 1) indicated that each sample crystallized with the expected hackmanite structure. Each material contained some unreacted NaCl as an impurity phase with its content being less than 11

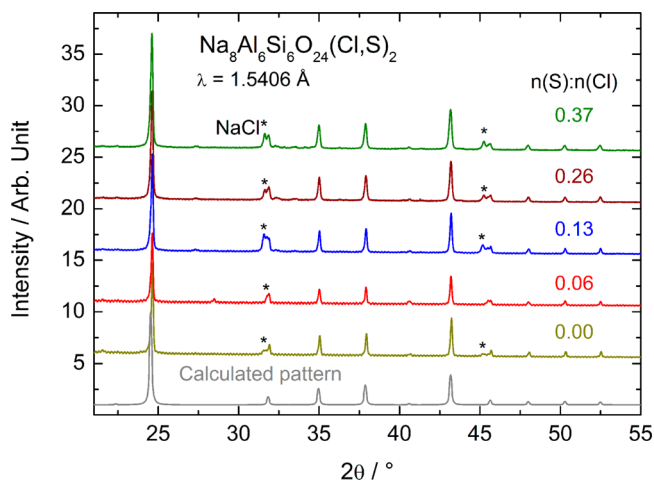


Figure 1. X-ray powder diffraction patterns of $\text{Na}_8\text{Al}_6\text{Si}_6\text{O}_{24}(\text{Cl},\text{S})_2$. The reference pattern was calculated with PowderCell²¹ from the structural data reported by Armstrong and Weller.⁸ The backgrounds were shifted for clarity.

wt % (Table 1). The unit cell volume increases slightly with increasing sulfur content (Table 1). In accordance with the

Table 1. Unit Cell Sizes, NaCl Impurity Contents as well as Nominal and Observed $n(\text{S}):n(\text{Cl})$ Ratios for $\text{Na}_8\text{Al}_6\text{Si}_6\text{O}_{24}(\text{Cl},\text{S})_2$. The Observed $n(\text{S}):n(\text{Cl})$ Values Have Been Corrected for the NaCl Content

no.	nominal $n(\text{S}):n(\text{Cl})$	a axis (Å)	V (Å ³)	NaCl content (w-%)	observed $n(\text{S}):n(\text{Cl})$
1	0.00	8.88688(2)	701.86	4	0.00
2	0.06	8.89442(2)	703.64	5	0.06
3	0.14	8.89259(2)	703.21	11	0.13
4	0.25	8.89747(2)	704.37	5	0.26
5	0.40	8.90187(2)	705.42	7	0.37

ionic radii, the S^{2-} ion is ca. 2% larger than Cl^- (i.e., 1.84 and 1.81 Å in 4-coordination,²⁰ respectively). Thus, such small increase in unit cell size is as anticipated and it can be taken as an indication of the sulfur entering the hackmanite lattice. It is impossible to say whether the sulfur is present as larger ions such as the disulfide S_2^{2-} rather than S^{2-} .

Because it is not possible to differentiate the Cl^- and S^{2-} ions from diffraction data as they have the same amount of electrons and they are similar in size, the chlorine and sulfur contents were probed with X-ray fluorescence measurements. The results indicated that the final materials have maintained the initial nominal $n(\text{S}):n(\text{Cl})$ ratio (Table 1). Thus, it was concluded that the prepared materials follow the intended stoichiometry.

3.2. Tenebrescence. The first functionality aimed for these materials was tenebrescence under UV irradiation from a low-cost hand-held UV lamp giving 254 or 365 nm emission. The intensity of color change in each material was quantified with reflectance measurements in the visible range (400–700 nm). The reflectance was first measured before UV irradiation and then after UV irradiation with the UV lamp. Finally, the difference of these two spectra was calculated to give the intensity of tenebrescence.

First, we investigated if any color change could be obtained for the present materials. With the 365 nm irradiation, no color change was achieved, whereas the 254 nm irradiation did yield tenebrescence of purple color. The reflectance difference curves (Figure 2) show a broad minimum centered at 550–560 nm and also that sulfur is needed to give the material tenebrescence. This is in agreement with earlier reports stating that the tenebrescence results from trapped electrons originating from sulfur.⁸ The most intense tenebrescence color was obtained with the $n(\text{S}):n(\text{Cl})$ ratio of 0.06 as confirmed with the naked eye, as well, whereas the material with no sulfur seemed to have lost some color during irradiation. The latter may be due to the uncertainty of the experimental setup, but from the photos (Figure 2) it seems that irradiation with 254 nm does make the material whiter (i.e., it bleaches some color centers). For the materials studied here, there is no straightforward correlation between the sulfur content and the intensity of the tenebrescence color, but it seems that the less there is sulfur the stronger is the color, provided that sulfur is present. Previously, Warner and Andersen²² reported that excessive insertion of sulfur in the hackmanite structure would destroy the tenebrescence and lead to a pale blue permanent color. Our materials thus seem to show a similar trend that the tenebrescence weakens with

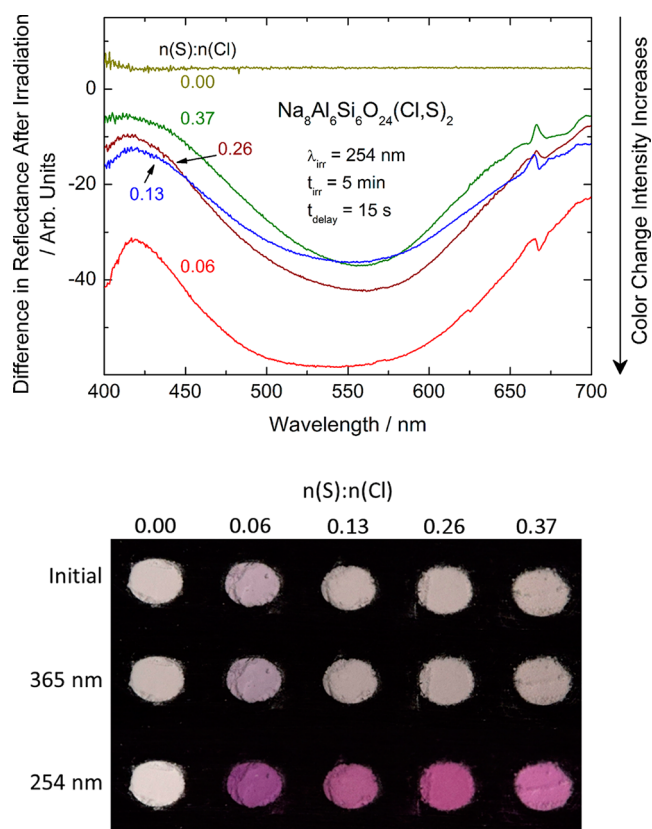


Figure 2. Intensity of color change for $\text{Na}_8\text{Al}_6\text{Si}_6\text{O}_{24}(\text{Cl},\text{S})_2$ after 254 nm irradiation. The photos show the initial color and those after 365 and 254 nm irradiation.

increasing sulfur content, but we observed no permanent color change toward blue.

Next, the persistence of the tenebrescence at room temperature was investigated under an incandescent light bulb (60 W, 20 cm distance) for $\text{Na}_8\text{Al}_6\text{Si}_6\text{O}_{24}(\text{Cl},\text{S})_2$ with $n(\text{S}):n(\text{Cl}) = 0.06$, which showed the most intense color change upon 254 nm UV irradiation. The color fades rather linearly during the first 5 h (Figure 3). After that, the fading becomes much slower, and the signal noise becomes significantly higher. To the naked eye, the material can hold

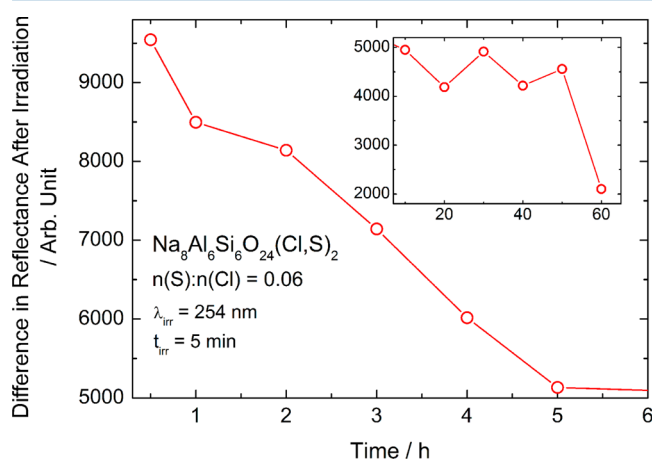


Figure 3. Fading of tenebrescence in $\text{Na}_8\text{Al}_6\text{Si}_6\text{O}_{24}(\text{Cl},\text{S})_2$ with $n(\text{S}):n(\text{Cl}) = 0.06$. The inset shows the fading after 10 h.

its color up to ca. 48 h, but at 60 h there is no color to be seen by the eye, even if the reflectance still indicates slight coloring.

3.3. UV Excited Luminescence. The second functionality aimed for these materials was luminescence under the hand-held UV lamp excitation at 254 and/or 365 nm. Luminescence was observed for all samples, but for $\text{Na}_8\text{Al}_6\text{Si}_6\text{O}_{24}(\text{Cl},\text{S})_2$ with $n(\text{S}):n(\text{Cl}) = 0.37$ only with 365 nm excitation and for $n(\text{S}):n(\text{Cl}) = 0.00$ only with 254 nm excitation (Figure 4).

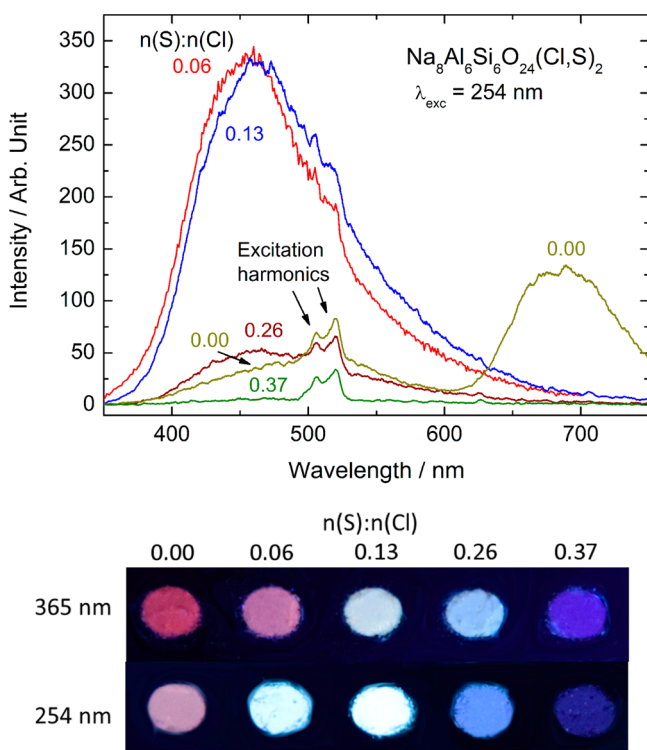


Figure 4. UV excited luminescence spectra of $\text{Na}_8\text{Al}_6\text{Si}_6\text{O}_{24}(\text{Cl},\text{S})_2$ with 254 nm excitation. The photos show the materials' color under 365 and 254 nm UV lamp excitation.

With 254 nm excitation, the main emission band is centered in the blue at 460 nm, and this was observed for all the materials showing luminescence. For the $n(\text{S}):n(\text{Cl}) = 0.00$ material, also a band in the red at 680 nm was observed. The most intense blue emission was obtained with $n(\text{S}):n(\text{Cl}) = 0.06$ and 0.13. With 365 nm excitation, a similar evolution was observed in the intensity of the blue emission, but the overall intensity for each sample was only 1% of that with 254 nm excitation (Figure S1). In contrast to excitation with 254 nm, the $n(\text{S}):n(\text{Cl}) = 0.26$ and 0.37 samples showed the red emission band, whereas the 0.00 sample gave no emission. When viewed with the naked eye, the samples with $n(\text{S}):n(\text{Cl}) = 0.00$, 0.26, and 0.37 show a completely different color under the two different UV excitations (Figure 4). This is a feature that could be utilized in optical marking.

Previously, Gaft et al.⁶ reported that the blue emission for natural hackmanites originates from s^2 type impurity ions. In the present case, no such impurities were detected by the XRF measurements. Instead, some 100 ppm of Fe, Ti, and Mn were detected from the zeolite starting material (see Table S2). These are known to be luminescence centers in many minerals.²³ However, since the present materials have rather little variation in their composition, there seems to be no plausible explanation for the strong variation of the blue

emission intensity between the samples in the series. That is, considering that emitting impurity ions would originate from one of the starting materials. On the other hand, it has been reported that NaCl can emit in the blue as well as change color, but these have been achieved only with higher-energy excitation than UV (i.e., VUV or X-rays).^{24,25} The emission of NaCl:S can be excited with UV, but then the luminescence is in the red (620 nm).²⁶ Furthermore, there is no correlation between the NaCl content of the samples (Table 1) and the intensity of luminescence (Figure 4) or tenebrescence (Figure 2). Therefore, we propose that the blue emission is due to structural defects in the final products. Strangely enough, the only sample showing red emission was that which contains no sulfur. This also contradicts the previous reports⁶ that the red emission would be due to S_2^- ions. All in all, the results indicate that a high Cl^- content is required for efficient emission, but some sulfur is needed nevertheless. Thus, it seems that sulfur acts as a sensitizer for the defect emission.

3.4. Persistent Luminescence. The third functionality aimed for these materials was persistent luminescence induced by the hand-held UV lamp with either 254 or 365 nm irradiation. To test this, we irradiated each sample for 30 min and recorded the emission spectrum in the dark, 1 min after turning off the lamp and thereafter in 1 min intervals.

It was possible to get considerable persistent luminescence with both 254 and 365 nm irradiation from all the samples that contained sulfur (Figures 5 and 6). The persistent emission has

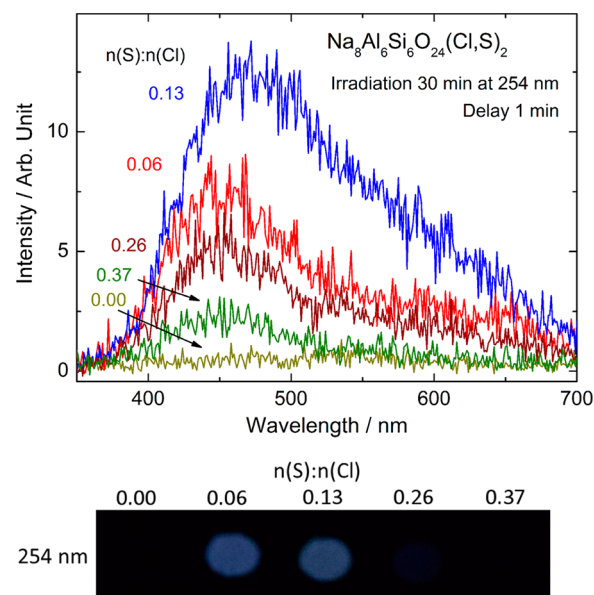


Figure 5. Persistent luminescence of $\text{Na}_8\text{Al}_6\text{Si}_6\text{O}_{24}(\text{Cl},\text{S})_2$ with 254 nm irradiation.

the same spectral shape and position as the blue UV excited luminescence. Thus, it should originate from the same luminescent centers. Considering intensity 1 min after removing the irradiation lamp, with 365 nm irradiation, the persistent luminescence intensity increases with decreasing sulfur content, whereas with 254 nm irradiation, the sulfur content $n(\text{S}):n(\text{Cl}) = 0.13$ gives a stronger persistent luminescence than the 0.06 one. Irradiation with 365 nm results in stronger persistent luminescence than 254 nm. This is the reverse of the UV excited luminescence. Probably the regular UV excited luminescence weakens due to the trapping

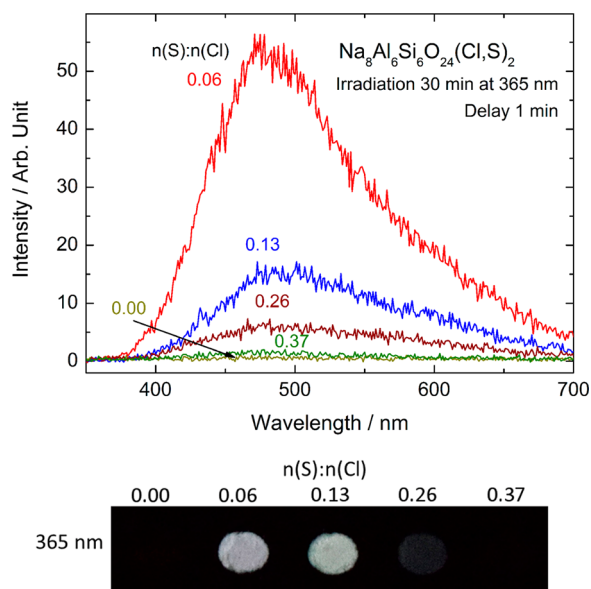


Figure 6. Persistent luminescence of $\text{Na}_8\text{Al}_6\text{Si}_6\text{O}_{24}(\text{Cl},\text{S})_2$ with 365 nm irradiation.

of energy with 365 nm irradiation. On the other hand, the 254 nm irradiation is not as eagerly trapped, and it is released as regular luminescence.

With $n(\text{S}):n(\text{Cl}) = 0.06$ and irradiation at 365 nm, the persistent luminescence lasts well up to 60 min (Figures 7 and

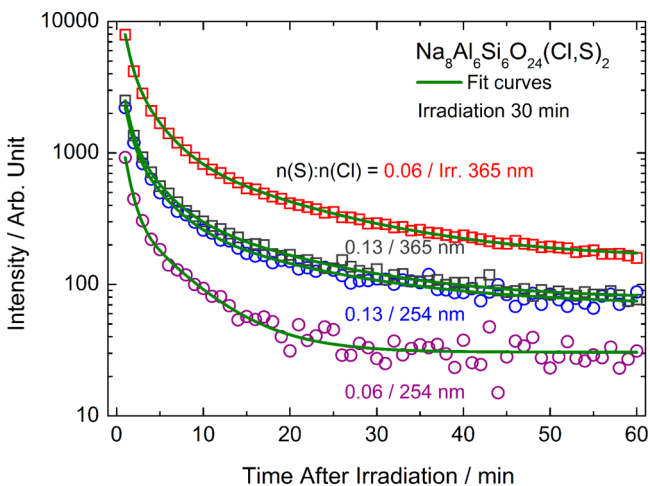


Figure 7. Fading of persistent luminescence for $\text{Na}_8\text{Al}_6\text{Si}_6\text{O}_{24}(\text{Cl},\text{S})_2$ with $n(\text{S}):n(\text{Cl}) = 0.06$ and 0.13 after 254 and 365 nm irradiation.

S2). With irradiation at 254 nm, the persistence is clearly shorter, but it reaches about 20 min anyway (Figures 7 and S3). A good persistence is observed also for the sample with $n(\text{S}):n(\text{Cl}) = 0.13$, but in this case the irradiation wavelength has very little effect on the time of persistence (Figures 7, S4, and S5). It is interesting to notice that the stronger persistent luminescence can be obtained with 365 nm, which produces no tenebrescence. Thus, the mechanism of persistent luminescence and tenebrescence are clearly different for the $\text{Na}_8\text{Al}_6\text{Si}_6\text{O}_{24}(\text{Cl},\text{S})_2$ materials. However, the detailed elucidation of this mechanism is out of the scope of the present paper.

The persistent luminescence spectra consist of at least two bands (i.e., the dominant one at 460 nm and another one at

570 nm). This suggests that at least two different types of defects participate in the emission process. Thus, to check number of possible luminescent centers (or eventually energy transfers), we made an exponential fit of the decay curve using eq 1:

$$I(t) = k_1 \exp(-t/\tau_1) + k_2 \exp(-t/\tau_2) + k_3 \exp(-t/\tau_3) + k_n \exp(-t/\tau_n) + \dots \quad (1)$$

where k = amplitude, t = time, and τ = lifetime. It was possible to obtain a good fit with a double exponential decay for the $n(\text{S}):n(\text{Cl}) = 0.06$ sample with 254 nm excitation, whereas a third component needed to be added for the other cases (eq 1). This indicates that there are probably at least three different luminescent centers participating in the persistent luminescence or an additional energy transfer between the two luminescent centers emitting at 460 and 570 nm.

The fit results (Table 2 and Figure 7) indicate that the first decay component is similar for all the samples, and it is equal to

Table 2. Persistent Luminescence Fading Times for $\text{Na}_8\text{Al}_6\text{Si}_6\text{O}_{24}(\text{Cl},\text{S})_2$

$n(\text{S}):n(\text{Cl})$	τ_1 (min)	τ_2 (min)	τ_3 (min)	τ_{av} (min)
$\lambda_{\text{exc}} = 254$ nm				
0.06	0.9 (± 0.04)	5.8 (± 0.3)	—	16.5 (± 0.1)
0.13	0.8 (± 0.06)	3.2 (± 0.4)	15.5 (± 2.8)	16.9 (± 0.1)
$\lambda_{\text{exc}} = 365$ nm				
0.06	0.7 (± 0.02)	2.8 (± 0.2)	14.5 (± 0.7)	14.8 (± 0.1)
0.13	0.7 (± 0.03)	2.9 (± 0.3)	14.0 (± 1.5)	16.8 (± 0.1)

ca. 1 min. The second component is from 3 to 6 min and the third ca. 15 min. The third component shows a decrease with increasing sulfur content. This suggests that the defects that need less thermal energy to release photons have the same character in all samples, and only the deeper traps that are related with the sulfur content and give longer persistent luminescence differ albeit not very much.

The persistent luminescence fading was further analyzed by determining the fading times as effective average decay times from the following equation.²⁷ eq 2:

$$\tau_{\text{av}} = \int I(t) t \, dt / \int I(t) \, dt \quad (2)$$

where $I(t)$ is intensity of luminescence at time point t and t is time. This quantity takes into account the whole fading curve, allowing the comparison of the overall decay characteristics of materials with different numbers of overlapping decay components. For $\text{Na}_8\text{Al}_6\text{Si}_6\text{O}_{24}(\text{Cl},\text{S})_2$, the τ_{av} values indicate that the decay is faster with 365 nm irradiation, but due to the brighter initial emission it is possible to observe it for longer time than with 254 nm irradiation. Furthermore, the τ_{av} values suggest that even with 254 nm irradiation, the material with $n(\text{S}):n(\text{Cl}) = 0.06$ shows a rather similar persistent luminescence decay than with 365 nm, even if it is not possible to fit a third component to the decay. Thus, it seems that the present materials possess a rather similar defect structure for trapping electrons with both 254 and 365 nm irradiation, but the trap densities (numbers of traps at similar energies) differ. This then affects the time of overall persistence.

Previously, there have been no reports on the persistent luminescence of hackmanites, although Gaft et al.⁶ stated that the luminescence of natural hackmanites may have a decay of a

few seconds. Persistent luminescence, however, is usually defined so that it should last at least some minutes. The observed 1 h duration for the present materials is very good, considering that no expensive, or any other, dopants were added. Tenebrescence has been reported for another persistent luminescence material, $\text{CaAl}_2\text{O}_4\text{:Eu}^{2+},\text{Nd}^{3+}$, but only using UV irradiation with high power density,²⁸ and we have observed the same using high-flux synchrotron X-rays. The fact that the present hackmanites can have both tenebrescence and persistent luminescence with a low-power hand-held UV lamp makes them far more attractive for practical applications than $\text{CaAl}_2\text{O}_4\text{:Eu}^{2+},\text{Nd}^{3+}$. Moreover, the present materials have these properties without expensive rare earth doping.

3.5. Structures of the Framework Cavities. Because both tenebrescence and persistent luminescence are due to structural defects, we carried out NMR and EPR measurements to probe local structures in the materials. For NMR, the ^{35}Cl signal was investigated because vacancies in the chloride sites are expected to act as the active sites for both phenomena. For the present $\text{Na}_8\text{Al}_6\text{Si}_6\text{O}_{24}(\text{Cl},\text{S})_2$ samples, the ^{35}Cl MAS NMR spectra show three different signals: at ca. -132 , -52 , and $+2$ ppm (Figure 8). There is very little shift between the samples

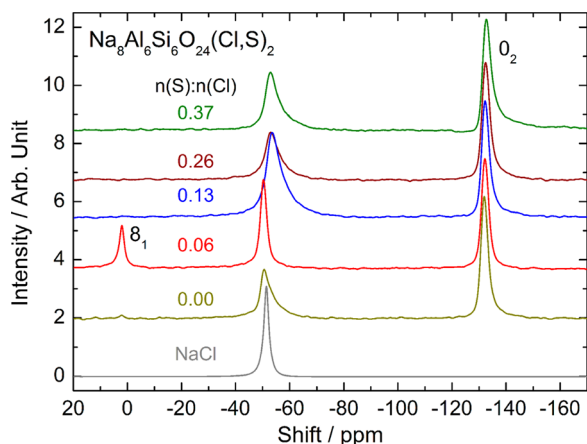


Figure 8. ^{35}Cl MAS NMR spectra of $\text{Na}_8\text{Al}_6\text{Si}_6\text{O}_{24}(\text{Cl},\text{S})_2$ and NaCl. The backgrounds were shifted for clarity.

for these signals, but the signal at $+2$ ppm is observed only for the samples with $n(\text{S}):n(\text{Cl}) = 0.00$ and 0.06 . For each sample, the signal at -52 ppm is due to the NaCl impurity (Figure 8).²⁹ However, the asymmetry and breadth of this line for all samples except that with $n(\text{S}):n(\text{Cl}) = 0.06$ suggest that there is another signal at ca. -58 ppm. It has been reported that the ^{35}Cl MAS NMR signal for the Cl^- ion in the tetrahedral $(\text{Na}_4\text{Cl})^{3+}$ entities of the sodalite structure is at -124 ppm.³⁰ Therefore, the strong signal at -132 ppm for the present materials indicates the presence of a high number of such framework cavities filled with chloride ions.

Previously, Trill et al.³⁰ have shown the applicability of NMR measurements in order to probe the total F center [i.e., $(\text{Na}_4)^{3+}$ entity] content as well as the number of F centers and their proximity around the studied nucleus. Trill et al.³⁰ used the m_n nomenclature to identify different NMR signals. In this nomenclature, m refers to the number of F center sites surrounding the studied nucleus and n refers to their proximity ("coordination sphere") from the studied nucleus. They reported the following values for a composition with 17% of F centers in the framework cavities: -123.9 ($m_n = \text{O}_2$), -116.2

(1_2) , -108.6 (2_2), -100.2 (3_2), -96.3 (1_1), -75.0 (2_1), -53.3 (3_1), and -32.6 ppm (4_1). In accordance with these values, we can assign the present signal at -132 ppm to a O_2 species, which is the regular vacancy-free signal of sodalite. The shoulder at -58 ppm is probably due to distorted NaCl species, even if there is a possibility that this could be a 3_1 center in the sodalite structure. Finally, the signal at 2 ppm can be assigned to chloride ions that have a rather high number of F centers in the first "coordination sphere" (e.g., Trill et al.³⁰ reported 9.9 ppm for a 8_1 species). This comes from the trend that with constant n , the ppm values increase with increasing m . It can be concluded that the vacancy structure in the present materials seems to be rather simple, uniform, and similar in each material.

To probe the presence of unpaired electrons, we carried out EPR measurements. Considering the ions present in the $\text{Na}_8\text{Al}_6\text{Si}_6\text{O}_{24}(\text{Cl},\text{S})_2$ materials (Na^+ , Al^{3+} , Si^{4+} , O^{2-} , Cl^- and $\text{S}^{2-}/\text{S}_2^{2-}$), we expect to observe EPR signals only if there are electrons in Cl^- vacancies (i.e., in the framework cavities). The measurements were carried out after irradiation with 254 nm to ensure the presence of such electrons.

We did not observe any EPR signals at room temperature, but with liquid helium cooling weak and wide signals around $g = 2.0$ were observed for samples with $n(\text{S}):n(\text{Cl}) = 0.00$ – 0.26 (Figure 9). There is no clear fine structure present, and the

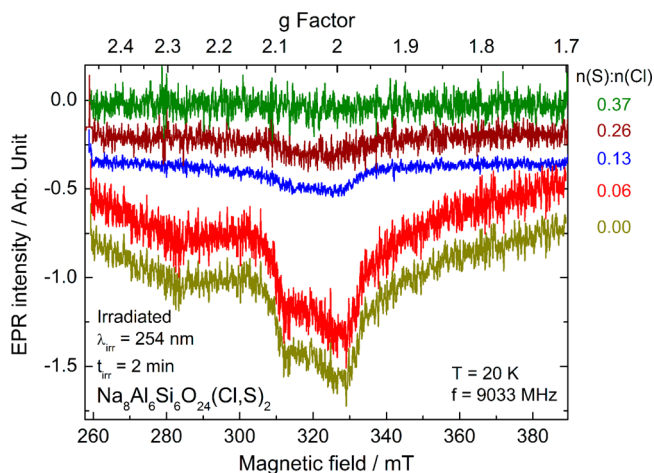


Figure 9. EPR spectra of irradiated $\text{Na}_8\text{Al}_6\text{Si}_6\text{O}_{24}(\text{Cl},\text{S})_2$ at 20 K.

shape of the signal is not the characteristic derivative. However, there seems a correlation between sulfur content and signal intensity so that lower S content gives a stronger signal, but with $n(\text{S}):n(\text{Cl}) = 0.00$ and 0.06 , the intensity is close to equal.

Hodgson et al.³¹ have reported that synthetic hackmanites show two EPR lines at g values 2.006 and 2.016 , when they are not in the colored form. They assigned the line at $g = 2.016$ to a sulfur species (another than the disulfide) and the line at 2.006 to an oxygen defect. After irradiation with UV and the coloration of the sample, a 13-line spectrum appears centered at $g = 2.002$. This is assigned to an electron trapped at a chlorine vacancy³¹ [i.e., the $(\text{Na}_4)^{3+}$ entity]. Although it was not possible to observe the 13 lines in the present work, the shape of the EPR curves suggests that there are multiple lines present. The fact that the EPR signal intensity increases with decreasing sulfur content in the $\text{Na}_8\text{Al}_6\text{Si}_6\text{O}_{24}(\text{Cl},\text{S})_2$ series can be explained by the pairing of electrons in neighboring $(\text{Na}_4)^{3+}$ entities close to sulfur. This means that the presence of the divalent sulfur decreases the number of unpaired electrons, and

thus the EPR signal obtainable from $(\text{Na}_4)^{3+}$ decreases. Finally, it is noteworthy that $(\text{Na}_4)^{3+}$ entities seem to be present even without sulfur. Thus, it seems that the framework cavities can be filled with electrons from other sources than sulfur (S_2^{2-}), as well. Of course, it is also possible that all or most of the EPR signals observed for each sample are due to intrinsic trapped electrons (i.e., F centers that exist already before the UV irradiation and that do not absorb visible wavelengths).

All in all, the NMR and EPR results showed no clear correlation between the intensity of tenebrescence or persistent luminescence and overall structures of the framework cavities. This means that the potential to exhibit both phenomena seems to be present in each material, but there is something more complicated than just the number or type of chlorine vacancies that controls their efficiency. This will be studied in more detail later using thermoluminescence and thermoluminescence excitation spectroscopy as well as probing the excitation and de-excitation of tenebrescence with reflectance spectroscopy.

4. CONCLUSIONS

Cubic $\text{Na}_8\text{Al}_6\text{Si}_6\text{O}_{24}(\text{Cl},\text{S})_2$ materials were successfully prepared with a solid state reaction. All materials containing sulfur were found to show purple tenebrescence, but the most intense color was obtained with a sulfur content $n(\text{S}):n(\text{Cl}) = 0.06$. For this material, the color persisted 2 days in a lit room at room temperature. Each material was also luminescent with the emission band maximum at 460 nm, but the overall color was dependent on the sulfur content. Considerable persistent luminescence peaking at 460 nm and persisting for 1 h was observed as well. To the knowledge of the authors, this is the first report of persistent luminescence for synthetic or natural hackmanites $\text{Na}_8\text{Al}_6\text{Si}_6\text{O}_{24}(\text{Cl},\text{S})_2$. These materials offer a very attractive alternative to produce low-cost persistent luminescence materials, since no expensive dopants are needed. The results suggested that there was a rather small amount of defects present to promote tenebrescence and persistent luminescence, and interestingly, the former is obtained with 254 nm while the latter is best with 365 nm irradiation. In the future, we will study the mechanism of both tenebrescence and persistent luminescence in these materials in more detail.

Finally, it must be noted that the present materials show a great versatility in their appearance under regular low-cost hand-held UV lamp and ordinary white light. This makes them very unique materials that could be used as multifunctional optical markers or sensors. For example, the materials with $n(\text{S}):n(\text{Cl}) = 0.13$ and 0.26 can show six different appearances in one material (Figure 10). Moreover, the materials presented here are very promising low-cost white/blue luminescent materials. Their use in practical applications such as white

LEDs, temperature sensors, and UV sensors will thus be studied further later on.

■ ASSOCIATED CONTENT

Supporting Information

The Supporting Information is available free of charge on the ACS Publications website at DOI: 10.1021/acs.inorgchem.5b00568.

UV excited emission spectra with 365 nm excitation and persistent luminescence spectra during fading, elemental contents of the starting materials as well as XPD, tenebrescence, photoluminescence, and luminescence data for washed samples (PDF)

■ AUTHOR INFORMATION

Corresponding Author

*E-mail: miklas@utu.fi.

Author Contributions

The manuscript was written through contributions of all authors. All authors have given approval to the final version of the manuscript.

Funding

Research leading to the present results was funded by Nordic Energy Research (AquaFEED project) and the Jenny and Antti Wihuri Foundation.

Notes

The authors declare no competing financial interest.

■ ACKNOWLEDGMENTS

Financial support from Nordic Energy Research (AquaFEED project) and Jenny and Antti Wihuri Foundation is gratefully acknowledged.

■ REFERENCES

- (1) Hölsä, J. *Electrochem. Soc. Interface* **2009**, 18, 42–45.
- (2) Lin, T.; Tang, Z.; Zhang, Z.; Wang, X.; Zhang, J. *J. Mater. Sci. Lett.* **2001**, 20, 1505–1506.
- (3) Matsuzawa, T.; Aoki, Y.; Takeuchi, N.; Murayama, Y. *J. Electrochem. Soc.* **1996**, 143, 2670–2673.
- (4) Pan, Z.; Lu, Y.-Y.; Liu, F. *Nat. Mater.* **2012**, 11, 58–63.
- (5) Medved, D. B. *Am. Mineral.* **1953**, 39, 615–629.
- (6) Gaft, M.; Panczer, G.; Nagli, L.; Yeates, H. *Phys. Chem. Miner.* **2009**, 36, 127–141.
- (7) Allen, T.; Renfro, N.; Nelson, D. *Gems & Gemology* **2014**, 50, 91–92.
- (8) Armstrong, J. A.; Weller, M. T. *Chem. Commun.* **2006**, 1094–1096.
- (9) Hassan, I.; Antao, S. M.; Parise, J. B. *Am. Mineral.* **2004**, 89, 359–364.
- (10) Peterson, R. C. *Can. Mineral.* **1983**, 21, 549–552.
- (11) Lee, O. I. *Am. Mineral.* **1936**, 21, 764–776.
- (12) Kirk, R. D. *Am. Mineral.* **1955**, 40, 22–31.
- (13) Hassib, A.; Beckman, O.; Annersten, H. *J. Phys. D: Appl. Phys.* **1977**, 10, 771–777.
- (14) Williams, E. R.; Simmonds, A.; Armstrong, J. A.; Weller, M. T. *J. Mater. Chem.* **2010**, 20, 10883–10887.
- (15) Goettlicher, J.; Kotelnikov, A.; Suk, N.; Kovalski, A.; Vitova, T.; Steiniger, R. Z. *Kristallogr. - Cryst. Mater.* **2013**, 228, 157–171.
- (16) Rietveld, H. M. *J. Appl. Crystallogr.* **1969**, 2, 65–71.
- (17) Rodriguez-Carvajal, J., *FullProf.2k (FullProf.2k (Version 5.30 - Mar2012))*; Laboratoire Leon Brillouin (CEA-CNRS): Gif-sur-Yvette, France, 2012.
- (18) Hubbard, C. R.; Snyder, R. L. *Powder Diff.* **1988**, 3, 74–77.

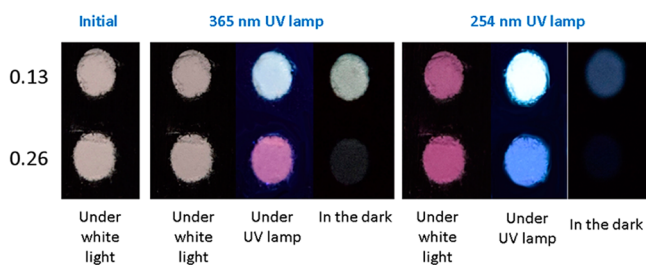


Figure 10. Appearance of $\text{Na}_8\text{Al}_6\text{Si}_6\text{O}_{24}(\text{Cl},\text{S})_2$ materials with $n(\text{S}):n(\text{Cl}) = 0.13$ and 0.26 under different lighting conditions.

- (19) International Centre for Diffraction Data, PDF-4+ 2013, entries 01-079-0091 (sodalite) and 01-080-3939 (NaCl).
- (20) Shannon, R. D. *Acta Crystallogr., Sect. A: Cryst. Phys., Diff., Theor. Gen. Crystallogr.* **1976**, *32*, 751–767.
- (21) Kraus, W.; Nolze, G. *PowderCell for Windows*, version 2.4., Federal Institute for Materials Research and Testing: Berlin, Germany, 2000.
- (22) Warner, T. E.; Andersen, J. H. *Phys. Chem. Miner.* **2012**, *39*, 163–168.
- (23) Gaft, M.; Reisfeld, R.; Panczer, G. *Modern Luminescence Spectroscopy of Minerals and Materials*; Springer: Berlin, Germany, 2005.
- (24) Ikezawa, M.; Kojima, T. *J. Phys. Soc. Jpn.* **1969**, *27*, 1551–1563.
- (25) Rodriguez-Lazcano, Y.; Correcher, V.; Garcia-Guinea, J. *Radiat. Phys. Chem.* **2012**, *81*, 126–130.
- (26) Ye, R.; Ohta, K.; Baba, M.; Nishidate, K. *Opt. Rev.* **1999**, *6*, 82–87.
- (27) Berberan-Santos, M. N.; Bodunov, E. N.; Valeur, B. *Chem. Phys.* **2005**, *315*, 171–182.
- (28) Ueda, U.; Shinoda, T.; Tanabe, S. *Opt. Mater. Express* **2013**, *3*, 787–793.
- (29) Stebbins, J. F.; Du, L.-S. *Am. Mineral.* **2002**, *87*, 359–363.
- (30) Trill, H.; Eckert, H.; Srdanov, V. *Phys. Rev. B: Condens. Matter Mater. Phys.* **2005**, *71*, 014412-1–014412-6.
- (31) Hodgson, W. G.; Brinen, J. S.; Williams, E. F. *J. Chem. Phys.* **1967**, *47*, 3719–3723.